Int. J. Solids Structures Vol. 27, No. 14, pp. 1773–1788, 1991
Printed in Great Britain

0020–7683/91 $3.00 + .00
Pergamon Press plc

DELAMINATION GROWTH AND BUCKLING IN AN ORTHOTROPIC STRIP

ERDOGAN MADENCI
Department of Aerospace and Mechanical Engineering, University of Arizona, Aero Building 16, Tucson, AZ 85721, U.S.A.

(*Received* 28 *December* 1989; *in revised form* 28 *August* 1990)

Abstract—This study presents an analytical solution to the problem of delamination growth and buckling in an orthotropic strip. Growth of an initially imperfect delamination located in the mid-plane of the strip is addressed when the applied stress is below the bifurcation point. The results for the buckling stress are also provided in the case of perfect delamination surfaces. Delamination growth and buckling is a commonly observed failure mode in laminated structures; this type of failure mode may cause structural degradation or stiffness reduction and leads ultimately to premature failure at stresses well below the design levels for an undamaged laminate. Under compression loading, the nature of the delamination response, which involves the interaction of delamination growth and buckling, is addressed by employing the governing equations of elastic stability under plane strain assumptions. Solutions to the problem of an orthotropic strip with a through-width delamination subjected to uniaxial compression are obtained by using mathematical techniques appropriate for mixed boundary value problems.

1. INTRODUCTION

Fiber-reinforced composite laminates are widely used in aircraft and space structures because of their high strength-to-weight ratio. In order to design laminated composite structures according to damage tolerance requirements, it is important to predict and understand their behavior under various load conditions. It is well known that laminated structures are prone to defects such as broken fibers, cracks in the matrix material, and interface delaminations. Premature failure due to the existence of delaminations is one of the most common failure modes in composite materials and bonded joints. Delaminations may arise as a result of imperfections during the manufacturing process (inclusions, wrinkles, or gas bubbles) or because of the effect of certain factors during the operational life of the laminate, such as low-velocity impact by foreign objects.

The presence of delaminations may cause structural degradation or stiffness reduction and leads ultimately to premature failure at stresses well below the design levels for an undamaged laminate. The response of delaminations in composites under shear loading has been addressed to a considerable extent within the realm of continuum mechanics. However, under compression loading the nature of the delamination response involves the interaction of delamination growth and buckling. Therefore, understanding the basic mechanics of the delamination response under a compressive load becomes essential in assessing the structural integrity of composite materials.

In recent years, delamination buckling and growth has been studied by many researchers in the field (Kachanov, 1976; Chai *et al.*, 1981; Bottega and Maewal, 1983; Polilov and Rabotnov, 1983; Yin and Wang, 1984; Yin *et al.*, 1984; Simitses *et al.*, 1984; Wang *et al.*, 1985a,b; Sallam and Simitses, 1985; Chai and Babcock, 1985; Ilic and Williams, 1986; Vizzini and Lagace, 1987; Storakess and Andersson, 1988; Bruno, 1988; Partridge *et al.*, 1989; Kachanov, 1988). However, these investigations employ structural mechanics theories such as those for beams and plates, and therefore entail approximations. First, in order to model the delaminated layer as a beam or as a plate, the ratio of delamination length to its thickness must be large. Second, the edges of the delamination are assumed to be either clamped or simply supported, and the delamination cannot grow unless the delaminated layer buckles. While suitable for initial strength evaluation of the delaminated composites, such approximations do not permit a detailed fracture mechanics examination. As a result, delamination growth in these studies is determined either by

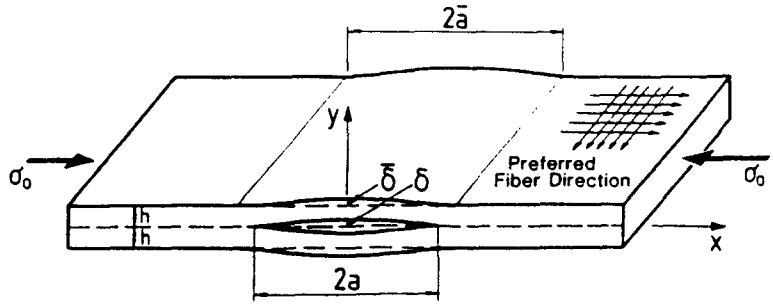

Fig. 1. Orthotropic strip with delamination under compression.

enforcing a global energy balance of the system or by incorporating the concept of energy release rate after the buckling point is reached.

Madenci (1987) and Madenci and Westmann (1989) studied the problem of delamination buckling and growth in a layered isotropic structure by employing the stability equations of elasticity theory which overcome these limitations. Based on the formulation presented by Madenci (1987), this study addresses the buckling and growth of an initially imperfect through-width delamination in an orthotropic strip subjected to a compressive load (up to the buckling point). The detailed fracture mechanics examination is achieved by allowing the delaminated region to be slightly open. This approach permits the study of the growth process which might eventually lead to buckling.

Section 2 presents the mathematical model for uniaxial in-plane loading when the delamination and bounding surfaces are slightly perturbed from the perfect configuration. In Section 3, the solution is obtained by first reducing the problem to a pair of dual integral equations and then to the solution of a single nonhomogeneous Fredholm integral equation of the second kind. The solution to this equation provides the stress intensity factor for applied compressive stress under a specified delamination thickness. The stress intensity factor is determined to be a complex function of the applied stress, unlike those usually encountered in linear elastic fracture mechanics. Allowing the slight perturbation of the surfaces to disappear results in a homogeneous Fredholm integral equation of the second kind. The solution to this equation provides the buckling stress and the mode shape for a specified delamination thickness.

Section 4 outlines the numerical method used to solve these equations. Numerical results are presented to show how the buckling stress and the stress intensity factor depend on the applicable parameters.

2. PROBLEM STATEMENT

This study is concerned with the growth and buckling of a delamination embedded in a flat orthotropic strip subjected to in-plane compressive loads. The principal axes of the material symmetry are taken to be the same as the reference coordinate system (x, y, z) in which the symmetry plane $y = 0$ coincides with the mid-surface of the layer (Fig. 1). This strip, infinite in length, has unit width and thickness $2h$. A through-width delamination of length $2a$ ($a = 1$) is located in the mid-plane of the strip.† The bounding and delamination surfaces $\bar{S}$ and S, respectively, can be expressed as

$$\bar{S} = \{x, y+\bar{\Delta}(x), z : x \in [0, \infty), y = \pm h, z \in [0, 1]\}$$

$$S = \{x, y+\Delta(x), z : x \in [0, \infty), y = \pm 0, z \in [0, 1]\}.$$

The initially imperfect bounding and delamination surfaces, which deviate only slightly

† The half delamination length a is taken to be unity in order to achieve a dimensionless statement of the problem.

from the perfect configuration ($y = \pm h$, $y = 0$), can be described by the functions $\bar{\Delta}(x)$ and $\Delta(x)$, respectively:†

$$\bar{\Delta}(x) = \frac{\bar{\delta}}{2}\left(1+\cos\frac{\pi x}{a}\right)H(\bar{a}-x)$$

$$\Delta(x) = \frac{\delta}{2}\left(1+\cos\frac{\pi x}{a}\right)H(a-x). \tag{1}$$

The relationship between the primary parameters $\bar{\delta}$ and δ, the amplitudes of the imperfections, can be established from the constant volume requirement of the material and from the assumption that $\bar{a} = a+h$. This results in the relationship

$$\bar{\delta} = \frac{\delta}{a+h} \tag{2}$$

for the functions given in (1).

The strip is subjected to an in-plane compressive loading σ_0 resulting from the initial equilibrium state. In terms of the rectangular Cartesian components of the stress (σ_{ij}^0), this may be stated by

$$\begin{aligned} &\sigma_{xx}^0 = -\sigma_0 \\ &\sigma_{ij}^0 = 0 \quad \text{otherwise.} \end{aligned} \qquad i,j = x,y,z \tag{3}$$

Surfaces $\bar{S}$ and S remain traction free.

If the rectangular Cartesian components of the displacement vector of the buckled state are denoted by u_i, the equilibrium equations derived by Bolotin (1963), Flugge (1972) and Washizu (1975) for the adjacent equilibrium positions may be stated as‡

$$[\sigma_{ij} + \sigma_{jk}^0 u_{i,k}]_{,j} = 0 \quad i,j,k = x,y,z. \tag{4}$$

In eqn (4), σ_{ij}^0 is the spatially constant initial equilibrium stress described by eqn (3). In the derivation of equations of elastic stability concerning bifurcation, it is assumed that the unit normal to the bounding surfaces is perpendicular to the direction of the applied load and/or that uniform loading is achieved at every cross-section. If this assumption does not hold, the nature of the stability problem is altered.

When the unit normal, with components n_i, to the bounding surface is slightly disturbed from the perpendicular position to the direction of the applied load, then the components of the stress vector, T_i, acting on that surface are given by

$$T_i = (\sigma_{ij} + \sigma_{jk}^0 u_{i,k})n_j^0 + \sigma_{ij}^0(n_j - n_j^0) \tag{5}$$

where n_i^0 denotes the components of the unit normal to the plane along which the applied load acts.

In eqn (5), the term $(n_j - n_j^0)$ is related to the function $\Delta(x_i)$, which describes the slightly imperfect surface as§

† Here and in the following, $H(x)$ denotes the Heaviside step function.

‡ In the derivation of eqn (4), it is assumed that the displacement gradients are small, $|u_{i,j}| \ll 1$, and standard tensor notation for summation and derivatives is employed.

§ Due to slight deviation from the perfect configuration, it is assumed that the gradient $\Delta(x_i)$ is small, $|\Delta_{,i}| \ll 1$.

$$n_j - n_j^0 = -\Delta_j \quad j = x, y, z. \tag{6}$$

The strip is composed of a homogeneous, elastic and orthotropic material with elastic coefficients

$$C_{11} = \frac{E_1}{v}(1 - \nu_{23}\nu_{32})$$

$$C_{22} = \frac{E_2}{v}(1 - \nu_{13}\nu_{32})$$

$$C_{12} = C_{21} = \frac{E_1}{v}(\nu_{21} + \nu_{23}\nu_{31}) = \frac{E_1}{v}(\nu_{12} + \nu_{13}\nu_{32})$$

$$C_{66} = G_{12} \tag{7}$$

in which

$$v = (1 - \nu_{12}\nu_{31})(1 - \nu_{23}\nu_{32}) - (\nu_{21} + \nu_{23}\nu_{31})(\nu_{12} + \nu_{13}\nu_{32}).$$

The constants E_i and G_{ij} stand for the moduli of elasticity, and ν_{ij} are the Poisson's ratios. Under plane strain assumptions,† the constitutive relations become

$$\begin{aligned}
\sigma_{xx} &= C_{11}u_{x,x} + C_{12}u_{y,y} \\
\sigma_{yy} &= C_{21}u_{x,x} + C_{22}u_{y,y} \\
\sigma_{xy} &= C_{66}(u_{x,y} + u_{y,x}) \\
\sigma_{zz} &= \nu_{31}\sigma_{xx} + \nu_{32}\sigma_{yy} \\
\sigma_{xz} &= \sigma_{yz} = 0.
\end{aligned} \tag{8}$$

Substitution from eqn (1) into eqns (4) and (5) results in the governing differential equations for an orthotropic material under plane strain assumptions as

$$\begin{aligned}
(C_{11} - \sigma_0)u_{x,xx} + C_{66}u_{x,yy} + (C_{12} + C_{66})u_{y,xy} &= 0 \\
(C_{66} - \sigma_0)u_{y,xx} + C_{22}u_{y,yy} + (C_{12} + C_{66})u_{x,xy} &= 0.
\end{aligned} \tag{9}$$

The boundary conditions associated with the traction-free surface S then become

$$\left.\begin{aligned} C_{12}u_{x,x} + C_{22}u_{y,y} &= 0 \\ C_{66}(u_{x,y} + u_{y,x}) + \sigma_0\bar{\Delta}_{,x} &= 0 \end{aligned}\right\} \quad y = \pm h \quad x \in [0, \infty). \tag{10a, 10b}$$

The presence of symmetry with respect to the mid-plane ($y = 0$) and the requirement that the surface S (delamination) be traction free result in the following boundary conditions:

$$\left.\begin{aligned} C_{66}(u_{x,y} + u_{y,x}) + \sigma_0\Delta_{,x} &= 0 \\ C_{12}u_{x,x} + C_{22}u_{y,y} &= 0 \\ u_y &= 0 \end{aligned}\right\} \quad y = 0^+ \quad \begin{aligned} &x \in [0, \infty) \\ &x \in [0, 1) \\ &x \in (1, \infty). \end{aligned} \tag{11a, 11b, 11c}$$

Further, the far field regularity conditions require that

† The displacement component u_z and derivatives with respect to z vanish due to plane strain assumptions. Thus, u_x and u_y are only functions of x and y.

$$u_x, u_y \to 0 \quad \text{for} \quad y \in [0, h], \quad x \to \infty.$$

When the term $(n_i - n_i^0)$ in eqn (5) disappears (i.e. the boundaries are perfect, $\delta = 0$), then the nature of the boundary value problem changes; it becomes an instability problem. Its solution involves the search for σ_0 so that nontrivial solutions of eqn (2) exist subject to the boundary conditions that T_i [eqn (5)] vanish on $\bar{S}$ and S. It is worthwhile mentioning here that the effect of nonlinearities which may affect the growth of delamination near the bifurcation point is not reflected in the present analysis because of the assumptions involved in the derivation of eqns (4) and (5).

3. MATHEMATICAL FORMULATION AND SOLUTION

The solution procedure begins by applying the pair of Fourier sine and cosine transforms to the displacement components. These transformations are defined as

$$\bar{u}_x(\xi, y) = \int_0^\infty u_x(x, y) \sin(\xi x)\, dx$$

$$\bar{u}_y(\xi, y) = \int_0^\infty u_y(x, y) \cos(\xi x)\, dx \tag{12}$$

with the inversion

$$u_x(x, y) = \frac{2}{\pi} \int_0^\infty \bar{u}_x(\xi, y) \sin(\xi x)\, d\xi$$

$$u_y(x, y) = \frac{2}{\pi} \int_0^\infty \bar{u}_y(\xi, y) \cos(\xi x)\, d\xi. \tag{13}$$

The displacement equilibrium eqns (9), when transformed according to eqn (13), reduce to a pair of ordinary differential equations for $\bar{u}_x(\xi, y)$ and $\bar{u}_y(\xi, y)$,†

$$C_{66}\bar{u}_x''(\xi, y) - (C_{11} - \sigma_0)\xi^2 \bar{u}_x(\xi, y) - (C_{12} + C_{66})\xi \bar{u}_y'(\xi, y) = 0$$
$$C_{22}\bar{u}_y''(\xi, y) - (C_{66} - \sigma_0)\xi^2 \bar{u}_y(\xi, y) + (C_{12} + C_{66})\xi \bar{u}_x'(\xi, y) = 0. \tag{14}$$

Nontrivial solutions to eqns (14) are determined to be

$$\bar{u}_x(\xi, y) = \sum_{i=1}^{4} A_i(\xi) e^{r_i \xi y} \quad \text{and} \quad \bar{u}_y(\xi, y) = \sum_{i=1}^{4} B_i(\xi) e^{r_i \xi y} \tag{15}$$

in which $A_i(\xi)$ and $B_i(\xi)$ are related by

$$B_i(\xi) = k(r_i) A_i(\xi)$$

where

$$k(r) = \frac{C_{66} r^2 - (C_{11} - \sigma_0)}{(C_{12} + C_{66}) r}. \tag{16}$$

The parameters r_i $(i = 1, \ldots, 4)$ are the roots of the characteristic equation

† Prime denotes differentiation with respect to variable y.

$$r^4 - 2Pr^2 + Q = 0 \tag{17}$$

where

$$P = \frac{C_{22}(C_{11}-\sigma_0)+C_{66}(C_{66}-\sigma_0)-(C_{12}+C_{66})^2}{2C_{22}C_{66}}$$

and

$$Q = \frac{(C_{11}-\sigma_0)(C_{66}-\sigma_0)}{C_{22}C_{66}}.$$

The characteristic roots r_i of eqn (17) may either be real or complex, depending on the composite system, as mentioned by Elliott (1948) and Sih and Chen (1981). If $P^2 > Q$ and provided that $Q > 0$, then the roots are real:

$$r_1 = \alpha, \quad r_2 = -\alpha, \quad r_3 = \beta, \quad \text{and} \quad r_4 = -\beta$$

where

$$\alpha = \sqrt{P+\sqrt{P^2-Q}} \quad \text{and} \quad \beta = \sqrt{P-\sqrt{P^2-Q}}.$$

For $P^2 < Q$ and provided that $P > 0$, the roots become complex:

$$r_1 = \gamma + i\zeta, \quad r_2 = \bar{r}_1, \quad r_3 = -r_1, \quad \text{and} \quad r_4 = -\bar{r}_1$$

where

$$\gamma = \sqrt{\frac{\sqrt{Q}+P}{2}} \quad \text{and} \quad \zeta = \sqrt{\frac{\sqrt{Q}-P}{2}}.$$

The general solutions for $u_x(\xi, y)$ and $u_y(\xi, y)$ in the case of real roots are

$$\begin{aligned}
\bar{u}_x(\xi, y) &= A_1(\xi)\,e^{\alpha\xi y} + A_2(\xi)\,e^{-\alpha\xi y} + A_3(\xi)\,e^{\beta\xi y} + A_4(\xi)\,e^{-\beta\xi y} \\
\bar{u}_y(\xi, y) &= k(\alpha)[A_1(\xi)\,e^{\alpha\xi y} - A_2(\xi)\,e^{-\alpha\xi y}] + k(\beta)[A_3(\xi)\,e^{\beta\xi y} - A_4(\xi)\,e^{-\beta\xi y}]
\end{aligned} \tag{18}$$

and in the case of complex roots they become

$$\begin{aligned}
\bar{u}_x(\xi, y) &= [A_1(\xi)\,e^{\gamma\xi y} + A_2(\xi)\,e^{-\gamma\xi y}]\cos\zeta\xi y + [A_3(\xi)\,e^{\gamma\xi y} + A_4(\xi)\,e^{-\gamma\xi y}]\sin\zeta\xi y \\
\bar{u}_y(\xi, y) &= \{m[A_1(\xi)\,e^{\gamma\xi y} - A_2(\xi)\,e^{-\gamma\xi y}] + n[A_3(\xi)\,e^{\gamma\xi y} + A_4(\xi)\,e^{-\gamma\xi y}]\}\cos\zeta\xi y \\
&\quad - \{n[A_1(\xi)\,e^{\gamma\xi y} + A_2(\xi)\,e^{-\gamma\xi y}] - m[A_3(\xi)\,e^{\gamma\xi y} - A_4(\xi)\,e^{-\gamma\xi y}]\}\sin\zeta\xi y
\end{aligned} \tag{19}$$

where

$$m = \mathrm{Re}\,[k(\gamma+i\zeta)] \quad \text{and} \quad n = \mathrm{Im}\,[k(\gamma+i\zeta)].$$

The unknown coefficients A_1, A_2, A_3 and A_4 are to be determined from the boundary conditions (10), (11). Enforcement of the traction-free condition (10) on the surface $y = h$ and the shear-free condition (11) in the mid-plane $y = 0$ permits the expressions for A_1–A_3 in terms of A_4. The remaining unknown A_4 is determined by imposing the mixed boundary conditions (11b), (11c) in the plane of the delaminated region. Enforcing (11b), (11c) results in the following pair of dual integral equations:

$$\int_0^x C(\xi)\xi \cos(\xi x)\,d\xi = \int_0^x C(\xi)\xi G(\xi)\cos(\xi x)\,d\xi + f(x) \quad x \in [0, 1) \tag{20a}$$

$$\int_0^x C(\xi)\cos(\xi x)\,d\xi = g(x) \quad x \in (1, \infty) \tag{20b}$$

in which the unknown function $C(\xi)$ involves the remaining unknown A_4. The relationships between $C(\xi)$ and $A_4(\xi)$ and the known function $G(\xi)$ are given in the Appendix. The functions $f(x)$ and $g(x)$ which appear in the formulation as a result of the slight imperfections of the bounding surfaces are

$$f(x) = \delta \int_0^x [D_1(\xi)S_1(\xi) + D_2(\xi)S_2(\xi)]\xi \cos(\xi x)\,d\xi \tag{21a}$$

$$g(x) = \delta \int_0^x [D_3(\xi)S_1(\xi) + D_4(\xi)S_2(\xi)]\cos(\xi x)\,d\xi \tag{21b}$$

where the expressions for D_1–D_4, S_1 and S_2 are also given in the Appendix.

The dual integral eqns (20) are converted to a nonhomogeneous Fredholm integral equation of the second kind, as suggested by Sneddon and Lowengrub (1969), by means of the following integral representation for $C(\xi)$† (Copson, 1961):

$$C(\xi) = \delta\left[\int_0^1 t^{1/2}\Phi_1(t)J_0(\xi t)\,dt + \int_1^x t^{1/2}\Phi_2(t)J_0(\xi t)\,dt\right]. \tag{22}$$

In this representation, $\Phi_1(t)$ and $\Phi_2(t)$ are assumed to be continuous over the interval $[0, 1]$ and $[1, \infty]$, respectively, and are required to satisfy the conditions

$$\lim_{t \to 0^+} t^{1/2}\Phi_1(t) = 0 \quad \text{and} \quad \lim_{t \to \infty} t^{1/2}\Phi_2(t) = 0.$$

Substituting (22) into (20b) and utilizing the Weber-Schaftheitlin integral given by Watson (1944) leads to an Abel integral equation for $\Phi_2(t)$

$$\delta \int_x^\infty t^{1/2}\Phi_2(t)\frac{dt}{\sqrt{t^2 - x^2}} = g(x) \quad x \in (1, \infty). \tag{23}$$

Inverting eqn (23) by applying Abel's solution method presented by Whittaker and Watson (1920) and then substituting (21b) for $g(x)$ gives the final expression for $\Phi_2(t)$

$$\Phi_2(t) = \sqrt{2t}\int_0^\infty [D_3(\xi)S_1(\xi) + D_4(\xi)S_2(\xi)]\xi J_0(t\xi)\,d\xi \quad t \in (1, \infty). \tag{24}$$

Integration of (20a) within the limits of 0 to x and substitution from (22) into the left-hand side of the resulting equation with the use of the Weber–Schaftheitlin integral yields the second Abel integral equation

$$\delta \int_0^x t^{1/2}\Phi_1(t)\frac{dt}{\sqrt{x^2 - t^2}} = \int_0^x \left\{\int_0^\infty C(\xi)\xi G(\xi)\cos(\xi t)\,d\xi + f(t)\right\}dt \quad x \in [0, 1) \tag{25}$$

Applying Abel's solution method to invert the left-hand side of eqn (25) and then substituting from (22) and (21a) results in the final governing integral equation for $\Phi_1(t)$:

† In this paper, $J_\nu(x)$ denotes the Bessel function of the first kind, with argument x and order ν.

$$\Phi_1(t) = \int_0^\infty K(t,\tau;\sigma_0,h)\Phi_1(\tau)\,d\tau + L(t) \quad t\in[0,1) \tag{26}$$

where

$$K(t,\tau;\sigma_0,h) = \sqrt{t\tau}\int_0^\infty G(\xi)\xi J_0(t\xi)J_0(\tau\xi)\,d\xi$$

and

$$L(t) = \int_1^\infty K(t,\tau;\sigma_0,h)\Phi_2(\tau)\,d\tau + t^{1/2}\int_0^\infty [D_1(\xi)S_1(\xi)+D_2(\xi)S_2(\xi)]\xi J_0(t\xi)\,d\xi.$$

For the present problem, the stress intensity factor K_I along the delamination edge is obtained from the following expression:

$$\sigma_{yy}(x,0) = -\frac{2}{\pi}l\left\{\int_0^\infty \xi C(\xi)\cos(\xi x)\,d\xi - \int_0^\infty \xi G(\xi)C(\xi)\cos(\xi x)\,d\xi - f(x)\right\} \quad x\in(1,\infty) \tag{27}$$

in which $l = l(C_{11}, C_{12}, C_{22}, C_{66}, \sigma_0)$ and is given in the Appendix. Modifying (23) by integration by parts and substituting the resulting form into eqn (27) by use of the Weber–Schafheitlin integral yields the following:

$$\begin{aligned}\sigma_{yy}(x,0) = \frac{2}{\pi}l\delta\Bigg\{&[\Phi_1(1)-\Phi_2(1)]\left[\frac{x}{\sqrt{x^2-1}}-1\right]\\ &-\int_0^1 \frac{d}{dt}[t^{-1/2}\Phi_1(t)]\left[\frac{x}{\sqrt{x^2-t^2}}-1\right]dt + x^{-1/2}\Phi_2(x)\\ &-\int_1^x \frac{d}{dt}[t^{-1/2}\Phi_1(x)]\left[\frac{x}{\sqrt{x^2-t^2}}-1\right]dt + \int_0^1 t^{1/2}\Phi_1(t)\int_0^\infty \xi G(\xi)J_0(\xi t)\cos(\xi x)\,d\xi\,dt\\ &+\int_1^\infty t^{1/2}\Phi_2(t)\int_0^\infty \xi G(\xi)J_0(\xi t)\cos(\xi x)\,d\xi\,dt + f(x)\Bigg\} \quad x\in(1,\infty).\end{aligned} \tag{28}$$

All of the terms in eqn (28) except the first are bounded as x approaches 1.

Defining

$$\rho = x-1$$

and retaining the first term in (28) results in the near field solution for the normal stress:

$$\sigma_{yy}(x,0) = \frac{2}{\pi}l[\Phi_1(1)-\Phi_2(1)]\frac{\delta}{\sqrt{2\rho}} \quad \text{as } \rho\to 0^+. \tag{29}$$

From the well-known asymptotic expression for the normal stress in the vicinity of the delamination edge,

$$\sigma_{yy}(x,0) = \frac{K_I}{\sqrt{2\pi\rho}} \quad \text{as} \quad \rho \to 0^+ \tag{30}$$

where K_I is the stress intensity factor and ρ is the distance away from the delamination edge, the stress intensity factor for the present problem can be written as

$$K_I = \frac{2}{\sqrt{\pi}} l\delta[\Phi_1(1) - \Phi_2(1)]. \tag{31}$$

4. NUMERICAL RESULTS

For the problem under consideration, the general form of the integral equation is

$$\Phi(x) = \lambda \int_0^1 K(x, y; \sigma_0, h)\Phi(y)\,dy + F(x) \quad \lambda = 1. \tag{32}$$

The complexity of the kernels in eqn (26) requires that the integral equation be solved numerically. The procedure involves the reduction of the integral equation to a system of algebraic equations using Bode's rule for numerical quadrature provided by Abramowitz and Stegun (1972). As a result of this discretization, eqn (32) may be written as

$$\sum_{n=1}^{N+1} A_{mn}\Phi_n = F_n \quad m = 1, 2, \ldots, N+1 \tag{33}$$

in which

$$A_{mn} = \delta_{mn} - w_n K[(m-1)s, (n-1)s]$$

$$\Phi_n = \Phi[(n-1)s]$$

and

$$F_n = F[(n-1)s].$$

The integer N (divisible by 4) is the number of equal intervals of length s and the weights of Bode's rule denoted by w_n. This discretization results in $(N+1)$ equations in the $(N+1)$ unknowns $\Phi[(n-1)s]$.†

In the case of perfect bounding and delamination surfaces, $F(x)$ in (32) disappears, resulting in a system of homogeneous algebraic equations. A nontrivial solution of the integral equation is found by searching for those values of σ_0 which cause the determinant of A_{mn} to vanish. An increasing sequence of values of σ_0 is selected and the determinant of A_{mn} evaluated. Once a change in sign of the determinant is observed, a first estimate of the buckling stress is obtained by interpolation. This value is further refined by selecting values of σ_0 closely surrounding the initial estimate. This scheme was used successfully by Stahl and Keer (1972). The numerical evaluation of the infinite integrals in eqn (26) is carried out by using Bode's quadrature rule and a sufficient number of intervals is used to ensure the accuracy of results. Considerable care is taken in the evaluation of the infinite integrals as the integration parameter approaches 0 and ∞.

When the delamination edge is perpendicular to the fiber direction, the lamina properties for Modomor II/LY558 (graphite–epoxy) at a fiber-volume ratio of 0.67 are taken from Kriz and Stinchcomb (1979) as

† In the solution of eqn (26), the number of integration intervals is taken to be $N = 40$ as the result of a convergence study.

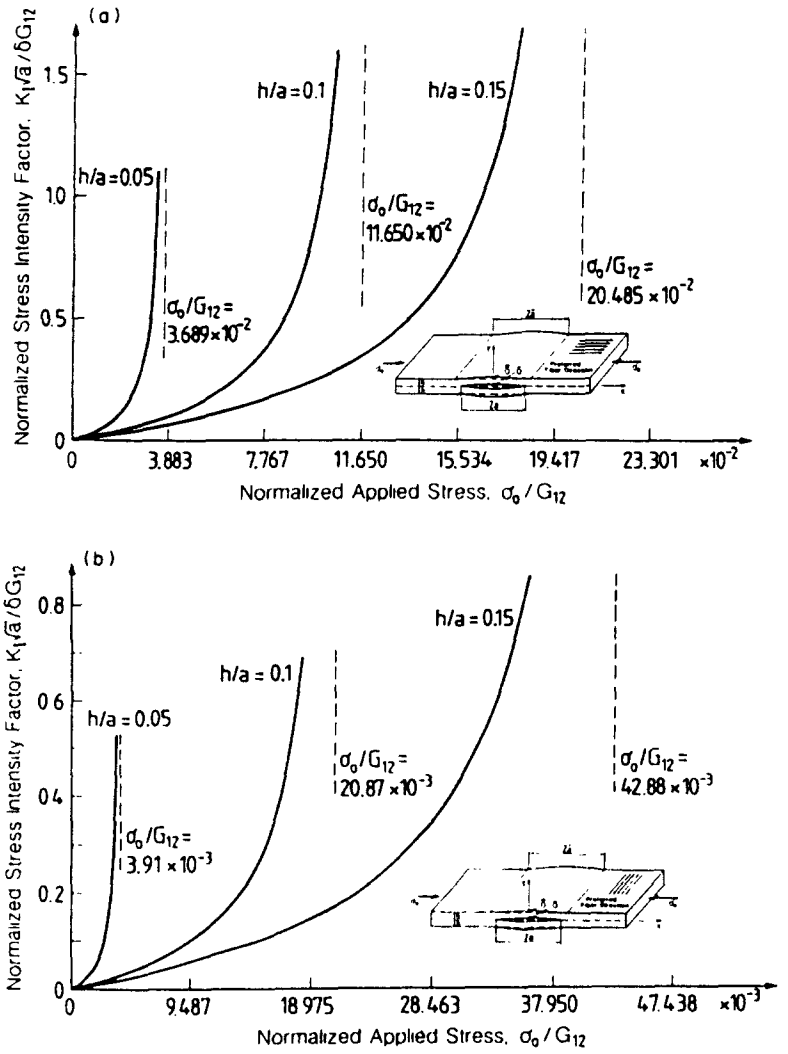

Fig. 2. Stress intensity factor as a function of applied stress. (a) Fibers parallel to loading direction. (b) Fibers perpendicular to loading direction.

$$E_1 = 22.8\times10^6\,\text{psi}; \quad G_{12} = G_{13} = 1.03\times10^6\,\text{psi}; \quad \nu_{12} = \nu_{13} = 0.3$$
$$E_2 = E_3 = 1.57\times10^6\,\text{psi}; \quad G_{23} = 0.527\times10^6\,\text{psi}; \quad \nu_{23} = 0.489,$$

resulting in real roots for the characteristic eqn (17). When the delamination edge is parallel to the fiber direction, the roots to eqn (17) become complex.

In the case of a slightly open delamination, the normalized stress intensity factor, $K_I\sqrt{a}/G_{12}\delta$, is calculated for a range of normalized applied stress $\sigma_0^* = \sigma_0/G_{12}$. The results are depicted in Fig. 2 for a specified dimensionless thickness, $h^* = h/a$. In order to identify the nature of the delamination growth process, the normalized stress intensity factor, $K_I\sqrt{h}/G_{12}\delta$, is calculated as a function of the dimensionless thickness, h^*, for a specified applied stress. This relationship is illustrated in Fig. 3 for a range of σ_0^* values. Asymptotes in Figs 2–4 indicate the buckling stress for the case of perfect delamination surfaces, i.e. $\delta = 0$.

In the case of a closed delamination, the solution procedure involves the search for σ_0 such that $\lambda = 1$ is an eigenvalue in eqn (26). The numerical treatment of the integral eqn (26) by the method outlined provides the variation of the dimensionless buckling stress, σ_0^*, as a function of the dimensionless thickness, h^* (Fig. 4). Once the buckling stress is computed, the buckling shape is obtained from the following expression:

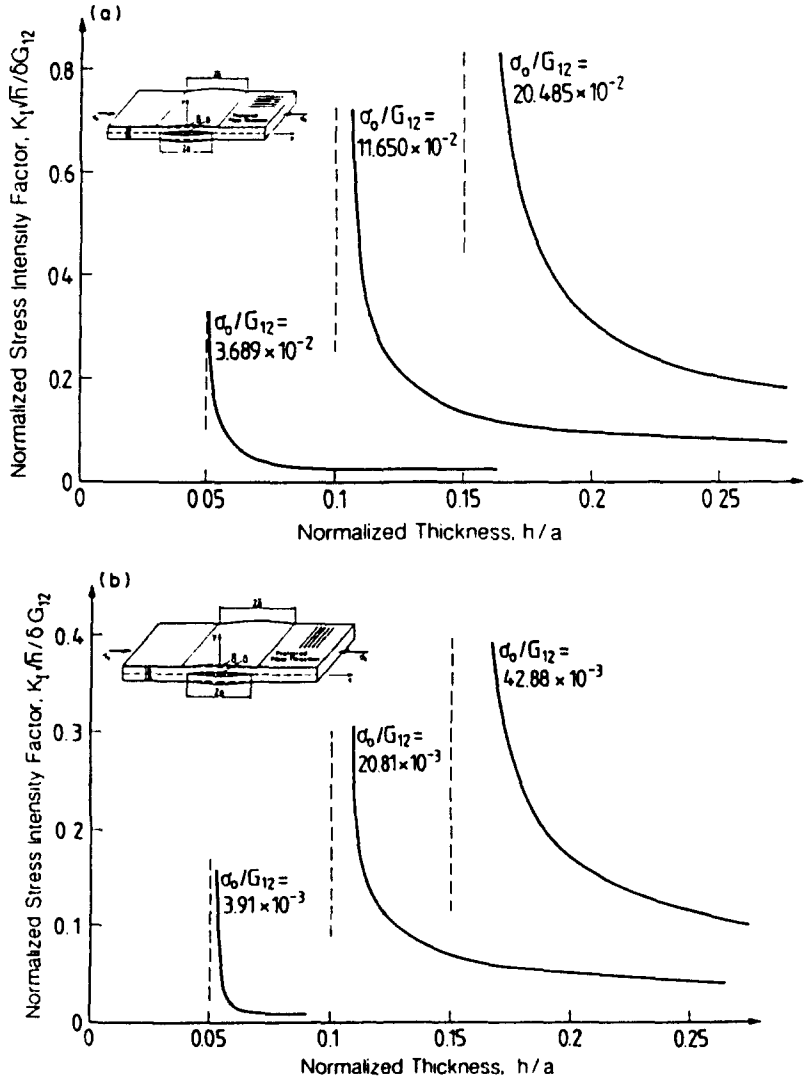

Fig. 3. Stress intensity factor as a function of thickness. (a) Fibers parallel to loading direction. (b) Fibers perpendicular to loading direction.

$$u_y(x,0) = \int_x^1 t^{1/2}\Phi_1(t)\frac{dt}{\sqrt{t^2-x^2}}. \tag{34}$$

The asymptotic form of eqn (33) is

$$u_y(x,0) = \Phi_1(1)\sqrt{1-x^2}+O[(1-x)] \quad \text{as } x\to 1^-.$$

A typical normalized buckling shape is presented in Fig. 5 for a dimensionless thickness $h^* = 0.1$.

5. FINAL COMMENTS

The present analysis focuses on the assessment of the delamination growth parameter, K_I, due to the slight opening of the delamination surfaces. Also, this is bounded by the results from the simplified model of a clamped and a simply supported thin plate analysis (Fig. 4). The results shown with dotted lines in Figs 4a–4b are approximated due to the numerical convergence difficulties encountered in the solution of the integral eqn (26) for $h^* < 0.05$.

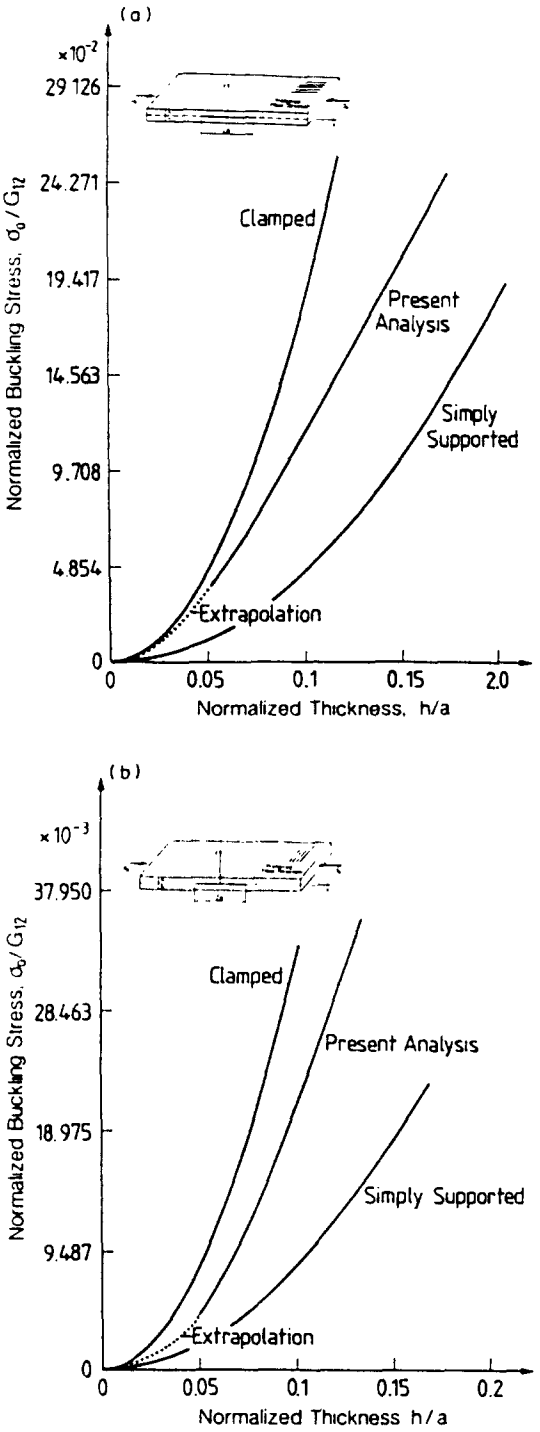

Fig. 4. Buckling stress as a function of thickness. (a) Fibers parallel to loading direction. (b) Fibers perpendicular to loading direction.

The stress intensity factors are determined to be a complex function of the applied stress, unlike those encountered in linear elastic fracture mechanics where the stress intensity factor is proportional to the applied load. For a specified amplitude, δ, of the initially imperfect delamination, should the stress intensity factor be greater than or equal to the interfacial fracture toughness† of the laminate, the present analysis indicates unstable delamination growth even before the buckling stress is reached. Recently, Pavier and

† In the open literature, a typical fracture toughness value for an epoxy system varies in the range 650–950 lb $in^{-3/2}$.

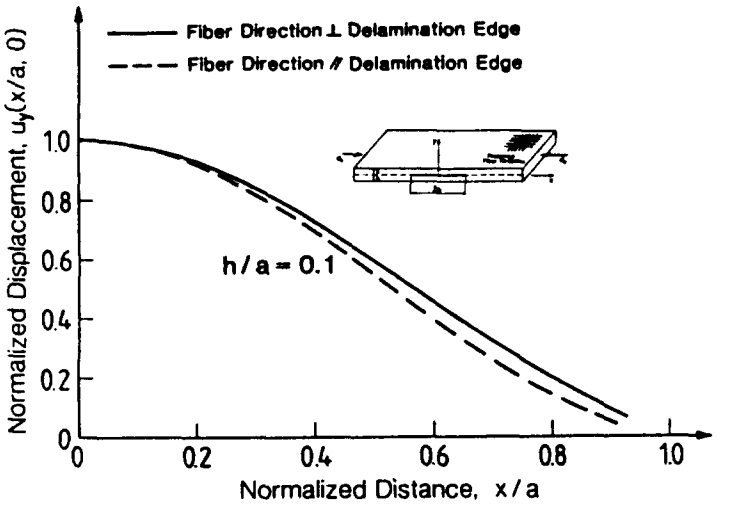

Fig. 5. Buckled delamination shape.

Chester (1990) experimentally found that delaminations in carbon fiber-reinforced epoxy tend to grow in size prior to failure due to buckling.

The study of delamination growth prior to buckling is made possible by determining the stress intensity factor. Previous analysis by other authors could not account for delamination growth before buckling. As shown in Fig. 3, the stress intensity factor increases for fixed delamination thickness under increasing applied stress. Once the interfacial fracture toughness is reached, then delamination growth occurs. As delamination grows, the stress intensity factor increases. This relationship is depicted for certain values of σ^* in Fig. 3. Once the delamination growth begins, it accelerates and the ratio of delamination length to thickness h^* decreases to the point that buckling occurs under the specified applied stress. As mentioned earlier, the problem of delamination response under compression involves the interaction between delamination growth and buckling, and this study represents an attempt toward a better understanding of this interaction.

Acknowledgements—This research was conducted while the author was serving as a Visiting Scientist at the Fraunhofer-Institute für Werkstoffmechanik, Freiburg, F.R.G.

REFERENCES

Abramowitz, M. and Stegun, I. A. (1972). *Handbook of Mathematical Functions*. Dover, New York.
Bolotin, V. V. (1963). *Nonconservative Problems of the Theory of Elastic Stability*. Macmillan, New York.
Bottega, W. J. and Maewal, A. (1983). Delamination buckling and growth in laminates. *J. Appl. Mech.* **50**, 184–189.
Bruno, D. (1988). Delamination buckling in composite laminates with interlaminar defects. *Theoret. Appl. Fract. Mech.* **9**, 145–159.
Chai, H. and Babcock, C. D. (1985). Two-dimensional modelling of compressive failure in delaminated laminates. *J. Comp. Mater.* **19**, 67–98.
Chai, H., Babcock, C. D. and Knauss, W. G. (1981). One dimensional modelling of failure in laminated plates by delamination buckling. *Int. J. Solids Structures* **17**, 1069–1083.
Copson, E. T. (1961). On certain dual integral equations. *Proc. Glasgow Math. Assoc.* **5**, 21–24.
Elliott, H. A. (1948). Three-dimensional stress distributions in hexagonal aeolotropic crystals. *Proc. Camb. Phil. Soc.* **44**, 522–533.
Flugge, W. (1972). *Tensor Analysis and Continuum Mechanics*. Springer, New York.
Ilic, S. and Williams, J. F. (1986). Compression failure modes in composites. *Theoret. Appl. Fract. Mech.* **6**, 121–127.
Kachanov, L. M. (1976). Separation of composite materials. *Polym. Mech.* **12**, 812–815.
Kachanov, L. M. (1988). *Delamination Buckling of Composite Materials*. Kluwer, The Netherlands.
Kriz, R. D. and Stinchcomb, W. W. (1979). Elastic moduli of transversely isotropic graphite fibers and their composites. *Exp. Mech.* **19**, 41–49.
Madenci, E. (1987). Local delamination buckling in layered structures. Ph.D. Thesis, University of California, Los Angeles.
Madenci, E. and Westmann, R. A. (1989). Local delamination buckling in layered systems. ASME, *J. Appl. Mech.* (accepted for publication).

Partridge, C., Waechter, R. T., Williams, J. F. and Jones, R. (1989). A finite element analysis of delamination behaviour in a circular laminate. *Comput. Struct.* **31**, 17–20.
Pavier, M. J. and Chester, T. W. (1990). Compression failure of carbon fiber-reinforced coupons containing central delaminations. *Composites* **21**, 23–31.
Polilov, A. N. and Rabotnov, N. Y. (1983). Development of layer separation upon compression of composites. *Izv. An SSSR Mekhanika Tverdoqa Tela* **18**, 165–171.
Sallam, S. and Simitses, G. J. (1985). Delamination buckling and growth of flat, cross-ply laminates. *Comp. Struct.* **4**, 361–381.
Sih, G. C. and Chen, E. P. (1981). *Cracks in Composite Materials*. Martinus Nijhoff, The Netherlands.
Simitses, G. J., Sallam, S. and Yin, W.-L. (1984). Effect of delamination on axially loaded laminated plates. *Proc. AIAA/ASME/ASCE/AHS 25th SDM Conf.*, Palm Springs, California, Paper 84-0964.
Sneddon, I. N. and Lowengrub, M. (1969). *Crack Problems in the Classical Theory of Elasticity*. John Wiley, New York.
Stahl, B. and Keer, L. M. (1972). Vibration and stability of cracked rectangular plates. *Int. J. Solids Structures* **8**, 69–81.
Storakess, B. and Andersson, B. (1988). Nonlinear plate theory applied to delamination in composites. *J. Mech. Phys. Solids* **36**, 689–718.
Vizzini, A. J. and Lagace, P. A. (1987). The buckling of a delaminated sublaminate on an elastic foundation. *J. Comp. Mater.* **21**, 1106–1117.
Wang, S. S., Zahlan, M. M. and Suemasu, H. (1985a). Compressive stability of delaminated random short fiber composites. Part I: Modeling and methods of analysis. *J. Comp. Mater.* **19**, 296–316.
Wang, S. S., Zahlan, M. M. and Suemasu, H. (1985b). Compressive stability of delaminated random short fiber composites. Part II: Experimental and analytical results. *J. Comp. Mater.* **19**, 317–333.
Washizu, K. (1975). *Variational Methods in Elasticity and Plasticity*. Pergamon Press, Oxford.
Watson, G. N. (1944). *A Treatise on the Theory of Bessel Functions*. Cambridge Univesity Press, U.K.
Whittaker, E. T. and Watson, G. N. (1920). *A Course of Modern Analysis*. Cambridge University Press, U.K.
Yin, W.-L., Sallam, S. and Simitses, G. J. (1984). Ultimate axial load capacity of a delaminated plate. *Proc. AIAA/ASME/ASCE/AHS 25th SDM Conf.*, Palm Springs, California, Paper 84-0892.
Yin, W.-L. and Wang, J. T. S. (1984). The energy release rate in the growth of a one-dimensional delamination. *J. Appl. Mech.* **51**, 939 941.

APPENDIX

Real roots

In eqn (20), the unknown function, $C(\xi)$, is related to the unknown coefficient, A_4, as follows:

$$C(\xi) = \frac{k(\alpha)[N_{14}(\xi)-N_{24}(\xi)]+k(\beta)[N_{14}(\xi)-N(\xi)]}{N(\xi)} A_4$$

where

$$N_{14}(\xi) = q(p-q)\,e^{-2(\alpha+\beta)2h} - 2pq\,e^{-(\alpha+\beta)2h} + q(p+q)\,e^{-2\alpha 2h}$$
$$N_{24}(\xi) = q(p-q) - 2pq\,e^{-(\alpha+\beta)2h} + q(p+q)\,e^{-2\beta 2h}$$
$$N_{14}(\xi) = -(p-q)\,e^{-2(\alpha+\beta)2h} - 2q\,e^{-(\alpha+\beta)2h} + (p+q)\,e^{-2\beta 2h}$$
$$N(\xi) = -(p-q) - 2q\,e^{-(\alpha+\beta)2h} + (p+q)\,e^{-2\alpha 2h}$$

in which

$$p = \frac{s(\beta)}{s(\alpha)} \quad \text{and} \quad q = \frac{t(\beta)}{t(\alpha)}.$$

The expressions for $s(r)$ and $t(r)$ are defined as

$$s(r) = C_{12} + C_{22} r k(r) \quad \text{and} \quad t(r) = C_{66}[r - k(r)].$$

The known function, $G(\xi)$, in the same equation is given as

$$G(\xi) = 1 + \frac{1}{l}\frac{s(\alpha)[N_{14}(\xi)+N_{24}(\xi)]+s(\beta)[N_{34}(\xi)+N(\xi)]}{k(\alpha)[N_{14}(\xi)-N_{24}(\xi)]+k(\beta)[N_{34}(\xi)-N(\xi)]}$$

where

$$l = \frac{s(\beta)-qs(\alpha)}{k(\beta)-qk(\alpha)}.$$

The functions $D_1(\xi)$ to $D_4(\xi)$ which appear in eqn (21) are defined as follows:

$$D_1(\xi) = \frac{s(\alpha)N_{11}(\xi) + s(\alpha)N_{21}(\xi) + s(\beta)N_{31}(\xi)}{lN(\xi)}$$

$$D_2(\xi) = \frac{s(\alpha)N_{12}(\xi) + s(\alpha)N_{22}(\xi) + s(\beta)N_{32}(\xi)}{lN(\xi)}$$

$$D_3(\xi) = -\frac{k(\alpha)N_{11}(\xi) - k(\alpha)N_{21}(\xi) + k(\beta)N_{31}(\xi)}{N(\xi)}$$

$$D_4(\xi) = -\frac{k(\alpha)N_{12}(\xi) - k(\alpha)N_{22}(\xi) + k(\beta)N_{32}(\xi)}{N(\xi)}$$

where

$$N_{11}(\xi) = -q\,e^{-(2\alpha+\beta)\xi h} - p\,e^{-\alpha\xi h}$$
$$N_{21}(\xi) = q\,e^{-\beta\xi h} - p\,e^{-\alpha\xi h}$$
$$N_{31}(\xi) = e^{-\beta\xi h} + e^{-(2\alpha+\beta)\xi h}$$
$$N_{12}(\xi) = (q+p)\,e^{-2\alpha\xi h}$$
$$N_{22}(\xi) = -(q-p)$$
$$N_{32}(\xi) = -2\,e^{-(\alpha+\beta)\xi h}.$$

In the same equation, the expressions for $S_1(\xi)$ and $S_2(\xi)$ are given as

$$S_1(\xi) = \frac{\pi}{2}\frac{a}{\bar{a}^2}\frac{\sigma_0}{t(\alpha)}\frac{1}{\xi}B(\xi, a) \quad \text{and} \quad S_2(\xi) = \frac{\pi}{2}\frac{1}{a}\frac{\sigma_0}{t(\alpha)}\frac{1}{\xi}B(\xi, a)$$

in which

$$B(\xi, c) = \int_0^c \sin\frac{\pi x}{c}\sin\xi x\,dx.$$

Complex roots

In eqn (20), the unknown function, $C(\xi)$, is related to the unknown coefficient, A_4, as follows:

$$C(\xi) = \frac{m[M_{14}(\xi) - M_{24}(\xi)] + n[M_{14}(\xi) + M(\xi)]}{M(\xi)}A_4$$

where

$$M_{14}(\xi) = p_2[t_2(\xi)S_1(\xi) - S_2(\xi)t_1(\xi)]\,e^{-2\gamma\xi h} + p_1[t_4(\xi)S_1(\xi) - S_4(\xi)t_1(\xi)]\,e^{-2\zeta\xi h} + p_2[t_4(\xi)S_2(\xi) - S_4(\xi)t_2(\xi)]\,e^{-4\gamma\xi h}$$
$$M_{24}(\xi) = p_1[t_4(\xi)S_1(\xi) - S_4(\xi)t_1(\xi)]\,e^{-2\gamma\xi h} + p_2[t_1(\xi)S_1(\xi) - S_1(\xi)t_1(\xi)] + p_2[t_1(\xi)S_4(\xi) - S_1(\xi)t_4(\xi)]\,e^{-2\gamma\xi h}$$
$$M_{34}(\xi) = p_2[t_1(\xi)S_2(\xi) - S_1(\xi)t_2(\xi)]\,e^{-2\gamma\xi h} + p_1[t_1(\xi)S_4(\xi) - S_1(\xi)t_4(\xi)]\,e^{-2\zeta\xi h} + p_1[t_2(\xi)S_4(\xi) - S_2(\xi)t_4(\xi)]\,e^{-4\gamma\xi h}$$
$$M(\xi) = p_1[t_3(\xi)S_1(\xi) - S_3(\xi)t_1(\xi)] + p_1[t_3(\xi)S_2(\xi) - S_3(\xi)t_2(\xi)]\,e^{-2\gamma\xi h} + p_2[t_2(\xi)S_1(\xi) - S_2(\xi)t_1(\xi)]\,e^{-2\gamma\xi h}$$

in which

$$t_1(\xi) = p_1\cos\zeta h\xi - p_2\sin\zeta h\xi; \quad t_2(\xi) = -p_1\cos\zeta h\xi - p_2\sin\zeta h\xi$$
$$t_3(\xi) = p_1\sin\zeta h\xi + p_2\cos\zeta h\xi; \quad t_4(\xi) = -p_1\sin\zeta h\xi + p_2\cos\zeta h\xi$$
$$S_1(\xi) = q_1\cos\zeta h\xi - q_2\sin\zeta h\xi; \quad S_2(\xi) = q_1\cos\zeta h\xi + q_2\sin\zeta h\xi$$
$$S_3(\xi) = q_1\sin\zeta h\xi + q_2\cos\zeta h\xi; \quad S_4(\xi) = q_1\sin\zeta h\xi - q_2\cos\zeta h\xi.$$

The constants p_1, p_2, q_1, and q_2 are defined as

$$p_1 = C_{66}(\gamma - m), \qquad p_2 = C_{66}(\zeta - n),$$
$$q_1 = C_{12} + C_{22}(\gamma m - \zeta n), \quad q_4 = C_{22}(\gamma n + \zeta m).$$

The known function, $G(\xi)$, in the same equation is given as

$$G(\xi) = 1 + \frac{1}{l}\frac{q_1[M_{14}(\xi) + M_{24}(\xi)] + q_2[M_{34}(\xi) - M(\xi)]}{m[M_{14}(\xi) - M_{24}(\xi)] + n[M_{34}(\xi) + M(\xi)]}$$

where

$$l = \frac{q_1p_2 - q_2p_1}{mp_2 - np_1}.$$

The functions $D_1(\xi)$ to $D_4(\xi)$ which appear in eqn (21) are defined as follows:

$$D_1(\xi) = \frac{q_1 M_{11}(\xi) + q_1 M_{21}(\xi) + q_2 M_{31}(\xi)}{lM(\xi)}$$

$$D_2(\xi) = \frac{q_1 M_{12}(\xi) + q_1 M_{22}(\xi) + q_2 M_{32}(\xi)}{lM(\xi)}$$

$$D_3(\xi) = -\frac{mM_{11}(\xi) - mM_{21}(\xi) + nM_{31}(\xi)}{M(\xi)}$$

$$D_4(\xi) = -\frac{mM_{12}(\xi) - mM_{22}(\xi) + nM_{32}(\xi)}{M(\xi)}$$

where

$$M_{11}(\xi) = -p_2 S_2(\xi) e^{-3\gamma\xi h} - p_1 S_3(\xi) e^{-\gamma\xi h}$$
$$M_{21}(\xi) = [p_2 S_1(\xi) - p_1 S_3(\xi)] e^{-\gamma\xi h}$$
$$M_{31}(\xi) = p_1 S_2(\xi) e^{-3\gamma\xi h} + p_1 S_1(\xi) e^{-\gamma\xi h}$$
$$M_{12}(\xi) = [t_1(\xi) S_2(\xi) - S_3(\xi) t_2(\xi)] e^{-2\gamma\xi h}$$
$$M_{22}(\xi) = t_1(\xi) S_3(\xi) - t_3(\xi) S_1(\xi)$$
$$M_{32}(\xi) = [t_2(\xi) S_1(\xi) - t_1(\xi) S_2(\xi)] e^{-2\gamma\xi h}.$$

In the same equation, the expressions for $S_1(\xi)$ and $S_2(\xi)$ become

$$S_1(\xi) = \frac{\pi}{2} \frac{a}{\bar{a}^3} \sigma_0 \frac{1}{\xi} B(\xi, a)$$

and

$$S_2(\xi) = \frac{\pi}{2} \frac{1}{\bar{a}} \sigma_0 \frac{1}{\xi} B(\xi, a).$$